RESEARCH/REVIEW ARTICLE

Middle to late Quaternary grain size variations and sea-ice rafting on the Lomonosov Ridge

Matt O'Regan, Emma Sellén & Martin Jakobsson

Department of Geological Sciences, Stockholm University, SE-106 91 Stockholm, Sweden

Keywords
Pleistocene; Lomonosov Ridge; grain size; sea ice.

Correspondence
Matt O'Regan, Department of Geological Sciences, Stockholm University, SE-106 91 Stockholm, Sweden.
E-mail: matt.oregan@geo.su.se

Abstract

Sea ice and icebergs are the dominant transport agents for sand-sized material to the central Arctic Ocean. However, few studies have investigated concurrent changes in the silt-sized fraction of Arctic sediments. Here we present an analysis of the coarse fraction content and silt grain size composition from middle and late Quaternary sediments recovered from the Lomonosov Ridge, in the central Arctic Ocean. A significant shift in the grain size record occurs at the marine isotope stage (MIS) 6/7 boundary, where larger amplitude variability in the sand fraction is seen in glacial and stadial periods. Below the MIS6/7 boundary, variations in the coarse fraction content are less pronounced, but prominent changes in the silt size fraction appear to define glacial and interglacial periods. Throughout the record, the percent weight of sortable silt in the fine fraction (SS % wt_{fines}), sortable silt mean size, and coarse silt content all increase as the >63 μm % wt content increases. This is consistent with observations of grain size spectra obtained from modern sea-ice samples, and indicates a strong overprint from sea ice on the silt distribution. The mechanism by which this sea-ice signal is preserved in the sediments across glacial and interglacial periods remains unclear. We suggest that the coarsening of silt-sized material during glacial periods could be attributed to either the entrainment of larger size fractions during suspension/anchor ice formation when sea levels are lowered, or diminished input and advection of fine fraction material during glacial periods.

In mid- to high-latitude settings, the abundance of terrigenous coarse-grained material (>63 μm) in sediments is commonly used as a proxy for the relative proportion of ice-rafted material (Polyak et al. 2010; Stein et al. 2012). The fine to coarse sand (63–2000 μm) fraction is widely used as an indication of iceberg related deposition, but the identification of sea-ice influenced deposition remains more problematic. Grain size distributions in modern sea ice are skewed towards the clay- and silt-sized range (Clark & Hanson 1983; Nürnberg et al. 1994; Reimnitz et al. 1998; Hebbeln 2000; Darby et al. 2009). This is interpreted to result from the entrainment of fine fraction material during suspension freezing. However, this process does not preclude the incorporation of sand-sized material (Pfirman et al. 1989). Furthermore, in contrast to suspension freezing, the formation of anchor ice, where the ice freezes to the bottom of the continental shelves, can also entrain a more poorly sorted and wider grain size spectrum (Reimnitz et al. 1987; Nürnberg et al. 1994; Darby et al. 2011). Although these entrainment processes indicate a potentially broad and diverse grain size spectrum in sea ice, modern sea-ice samples generally contain between 5 and 10% of sand-sized material (Clark & Hanson 1983; Darby et al. 2009; Dethleff & Kuhlmann 2010).

The large proportion and selective entrainment of fine fraction material in sea ice generates ambiguity in identifying the sea-ice rafted component of Arctic seafloor sediments. It also presents a challenge for identifying current related sorting of the fine fraction material. Unravelling the relative influence of different transport and sorting processes on Arctic sea floor sediments could greatly advance our understanding of sea ice and circulation changes in the geologic past. However, we still lack

Citation: *Polar Research* 2014, *33*, 23672, http://dx.doi.org/10.3402/polar.v33.23672

tightly calibrated age models for central Arctic sediments, that would allow detailed flux comparisons across glacial and interglacial periods, or between cores from different oceanographic settings (Backman et al. 2004; Alexanderson et al. 2014). In the absence of other age constraints, improving our ability to identify sea ice-rafted components of Arctic sediments can ultimately help constrain cylostratigraphic derived age models (O'Regan et al. 2008). Despite the recognized bias towards fine fraction entrainment in sea ice, there remains a notable absence of grain size data describing variations in the fine fraction component of Quaternary sediments from the central Arctic Ocean.

Here we present the first detailed look at variations in the silt fraction of middle and late Quaternary sediments from the circumpolar region of the Lomonosov Ridge. The records were generated on cores HLY0503-18JPC and HLY0503-18TC, recovered during the HOTRAX expedition in 2005 (Darby et al. 2005). The aim of the study is to investigate the relationship between silt distributions and the abundance of coarse-grained ice-rafted material and to determine if pronounced glacial and interglacial modes of sedimentation are recorded in the silt-sized fraction of sediments.

Regional setting and background

Cores HLY0503-18JPC and HLY0503-18TC were recovered from 2598 m water depth, in a ca. 2700 m deep Intra Basin on the Lomonosov Ridge (Fig. 1). Deep water (below 1700 m as defined by Jones 2001) from the Makarov Basin (Canada Basin Deep Water) flows

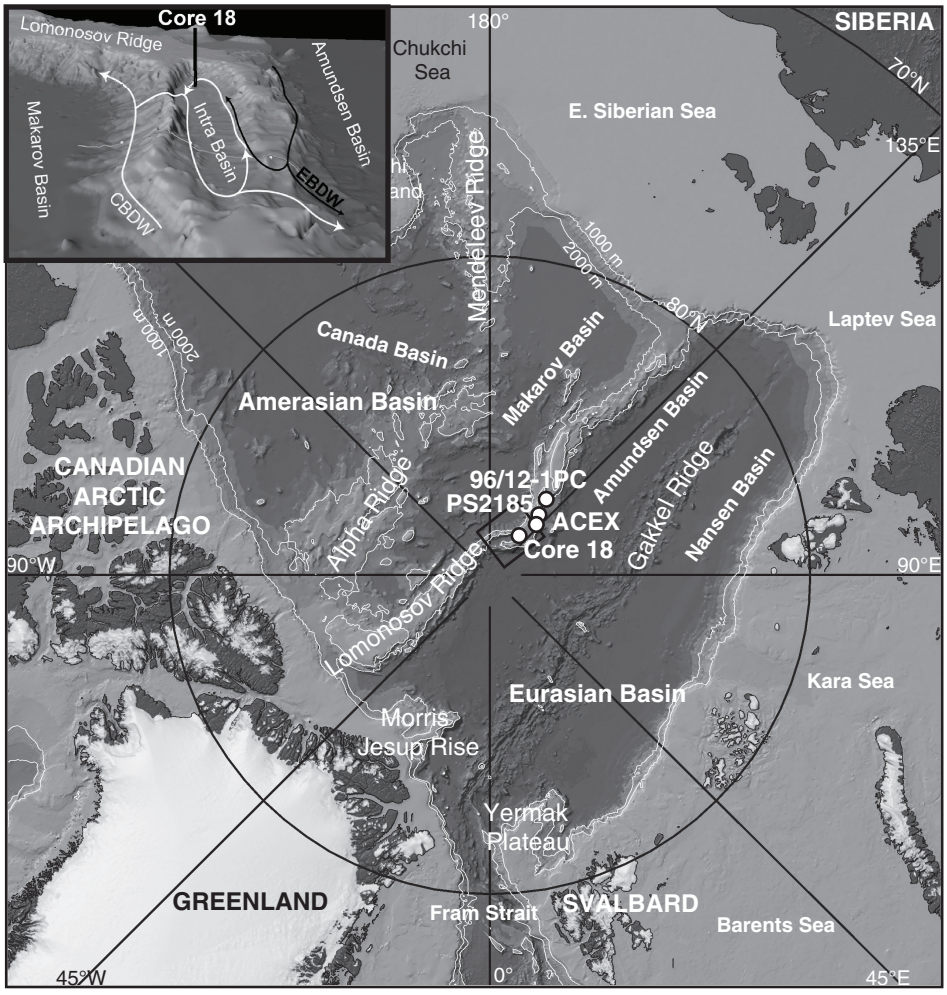

Fig. 1 Schematic map of the Arctic Ocean showing the site of Core 18, ACEX, 96/12-1PC and Ps-2185-6 on the Lomonosov Ridge. A three-dimensional image of the Intra Basin is shown in the top-left corner, with the paths of the Canadian Basin Deep Water (CBDW) and the Eurasian Basin Deep Water (EBDW) marked in grey and black, respectively. The bathymetry is from the International Bathymetric Chart of the Arctic Ocean, version 2.0 (Jakobsson et al. 2008).

Citation: *Polar Research* 2014, *33*, 23672, http://dx.doi.org/10.3402/polar.v33.23672

through the Intra Basin into the Amundsen Basin where it joins Eurasian Basin Deep Water and continues along the Lomonosov Ridge towards the Fram Strait (Björk et al. 2007). On the crest of the Lomonosov Ridge, at about 1000 m depth, the dominant water mass is instead the Upper Polar Deep Water (ca. 500–1700 m), which is slightly warmer and less dense than the underlying water mass (Jones 2001; Rudels et al. 2012).

Methods

The jumbo piston core HLY0503-18JPC and the trigger weight core HLY0503-18TC (88°27′N 146°34′E) were used in this study. The cores were retrieved from USCGC *Healy* during the HOTRAX expedition in 2005 (Darby et al. 2005). The piston core recovered 12.5 m sediment. The upper section of this core was dropped during core processing on the ship, and due to subsequent disturbances there is some stratigraphic uncertainty in the uppermost 2.14 m. In the composite section, the 1.9 m long trigger weight core replaces the top section of the piston core. The composite section made from these two cores is referred to as Core 18, and its depth scale referred to as metres composite depth (mcd). Sediments in Core 18 are composed of mainly fine-grained mud with silty and sandy layers. Interlaminated medium brown to dark brown layers are present throughout.

Grain size analysis

For the grain size analysis, a continuous set of 2 cm samples was taken from a u-channel. Sub-samples (3–4 g) of these were wet sieved through a 63-μm mesh. The sieving liquid was deionized water saturated with $CaCO_3$ in order to preserve calcareous microfossils. The coarse fraction was dried on the mesh in an oven and allowed to cool before weighing. The fine fraction (<63 μm) was collected in beakers where it was allowed to settle. The water was siphoned out and the samples were centrifuged. A dispersion liquid ($NaPO_3$) was added to the samples and they were thoroughly suspended using sonification. Each sample was analysed using 0.08 phi bin size divisions for the 1–63 μm fraction in the Sedigraph 5100 (Micromeritics, Norcross, GA, USA). The Sedigraph is based on the settling velocity principle and has been shown to provide reliable estimates of the sortable silt abundance and mean size when the % wt of sortable silt is >5% (Bianchi et al. 1999; McCave & Hall 2006; McCave et al. 2006). Although biogenic carbon was not removed, benthic and planktic foraminifera (Hanslik et al. 2010) and calcareous nannofossils (Backman et al. 2009) were only found in the upper 50 cm of the trigger weight core.

Silt statistical parameters (mean, sorting, skewness and kurtosis) were determined for the 2–63 μm size fraction using the GRADISTAT software (Blott & Pye 2001) and analysed using the original logarithmic (ϕ-scale) measures of Folk & Ward (1957). This approach was adopted to allow direct comparison with silt statistics reported for modern sea-ice samples collected in the Fram Strait (Dethleff & Kuhlmann 2010).

Age model

A stratigraphic correlation with the composite section from the Integrated Ocean Drilling Programs Expedition 302, the Arctic Coring Expedition (ACEX), was established using the multi-sensor core logging derived bulk density and magnetic susceptibility records, the alignment of key lithologic features, and in the upper few metres, variations in the coarse fraction content (Fig. 2). This correlation was previously published by Sellén et al. (2010), Hanslik et al. (2010) and Löwemark et al. (2012) and was not updated for this paper.

The stratigraphic correlation allows the Quaternary age model presented for the ACEX record (O'Regan et al. 2008) to be mapped onto Core 18 (Fig. 2). Beyond the last two glacial cycles, the ACEX age model was derived from cyclostratigraphic analysis of physical and environmental magnetic parameters down to the Bruhnes/Matuyama (B/M) boundary, and to palaeomagnetic excursion and subchron boundaries between the B/M and the Cobb Mountain Subchron (1215 Kya; O'Regan et al. 2008). Due to the lack of directly constrained chronostratigraphic markers, and continued uncertainty concerning the interpretation of apparent polarity reversals in High-Arctic sediments (Xuan et al. 2012) there remains considerable uncertainty in the derived chronology (Fig. 2). Despite these uncertainties, it is without doubt that the 8.1 m of sediment in Core 18 from below the base of MIS6 (Fig. 2) must span a number of glacial/interglacial periods during the middle part of the Pleistocene. Lithologically, the interglacial/interstadial sediments are recognized by being finer grained, bioturbated intervals with elevated Mn abundances (Jakobsson et al. 2000; O'Regan et al. 2008; Löwemark et al. 2012).

Results

Downhole and age-calibrated trends in grain size

The weight percent coarse fraction (>63 μm), weight percent sortable silt in the fine fraction (SS % wt_{fines}; 10–63 μm as defined by McCave, Manighetti, & Robinson 1995) and mean grain size of the fine fraction, all appear to have a

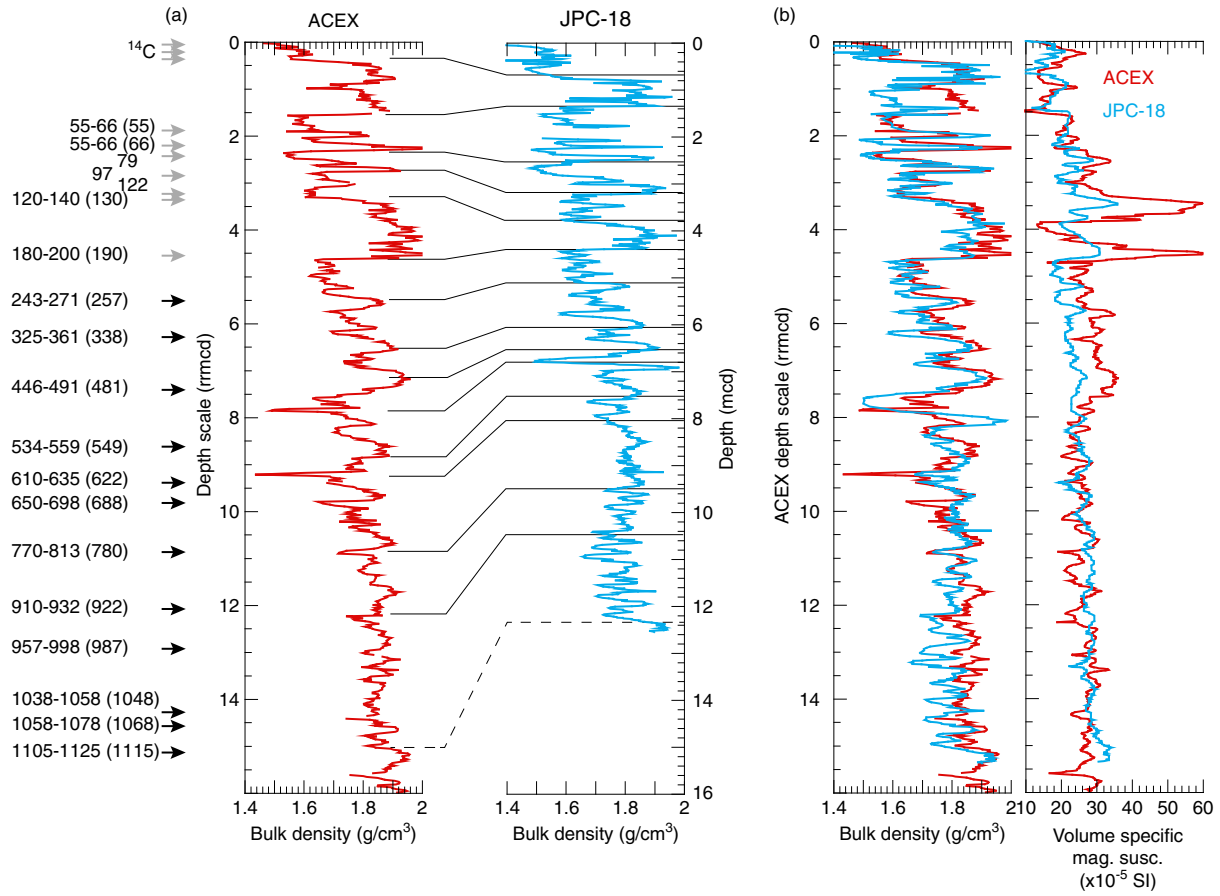

Fig. 2 (a) Correlation of bulk density between Core 18 and ACEX, and tie points used to develop the chronology of the ACEX record (O'Regan et al. 2008). In (b) the bulk density and magnetic susceptibility records from Core 18 are migrated onto the ACEX depth scale.

strong positive correlation with bulk density (Fig. 3). The weight percent clay-sized fraction (<2 μm) is inversely related. From the base of the record to ca. 4.4 mcd, there is more pronounced variation in the mean grain size of the fine fraction and SS % wt_{fines} than in the >63 μm % wt. Between 6.7 and 7 mcd, an anomalous interval occurs in Core 18, where a coarse lag deposit, originally interpreted as a possible erosional horizon during shipboard core description, is overlain by a very fine grained well sorted interval (Fig. 3). The same fine-grained interval is present in other cores from the Lomonosov Ridge, including the ACEX record where it stands out as a peach coloured clay layer surrounded by brown, bioturbated sediments (Expedition 302 Scientists 2006; O'Regan et al. 2008; Löwemark et al. 2012). Beginning at 4.4 mcd and continuing to the seafloor, there are a series of recurrent coarser grained intervals where the >63 μm % wt routinely exceeds 10–15% (Fig. 3).

Statistical parameters measured on the silt-sized fraction all exhibit trends consistent with variations in the mean grain size of the fine fraction and SS % wt_{fines}. Intervals with greater SS % wt_{fines} also exhibit lower values of kurtosis (flatter distributions), higher values for sorting (less sorted) and silt distributions that are positively (fine) skewed (i.e., they have a tail of finer material). The silt distributions within the coarse-grained intervals in the upper 4.4 mcd do not appear more poorly sorted than the coarser grained intervals below 4.4 mcd, but tend to be more strongly skewed (Fig. 3).

To illustrate how grain size variations change across the proposed glacial and interglacial periods, the same records are presented on the mapped ACEX age model (Fig. 4). Here it becomes apparent that through the earlier part of the record, mean grain sizes in the fine fraction and the SS % wt_{fines} both increase during glacial periods. Interpreted glacial age sediments also appear to have a flatter distribution, are more poorly sorted and finely skewed. All the silt-based parameters show a higher frequency variability than the >63 μm % wt. The sortable silt mean also seems to be lower during the shorter interglacial periods, and high during glacials. Notable offsets in these trends occur between ca. 500 and 800 Kya (Fig. 4; ca. 7–9.5 mcd,

Citation: *Polar Research* 2014, *33*, 23672, http://dx.doi.org/10.3402/polar.v33.23672

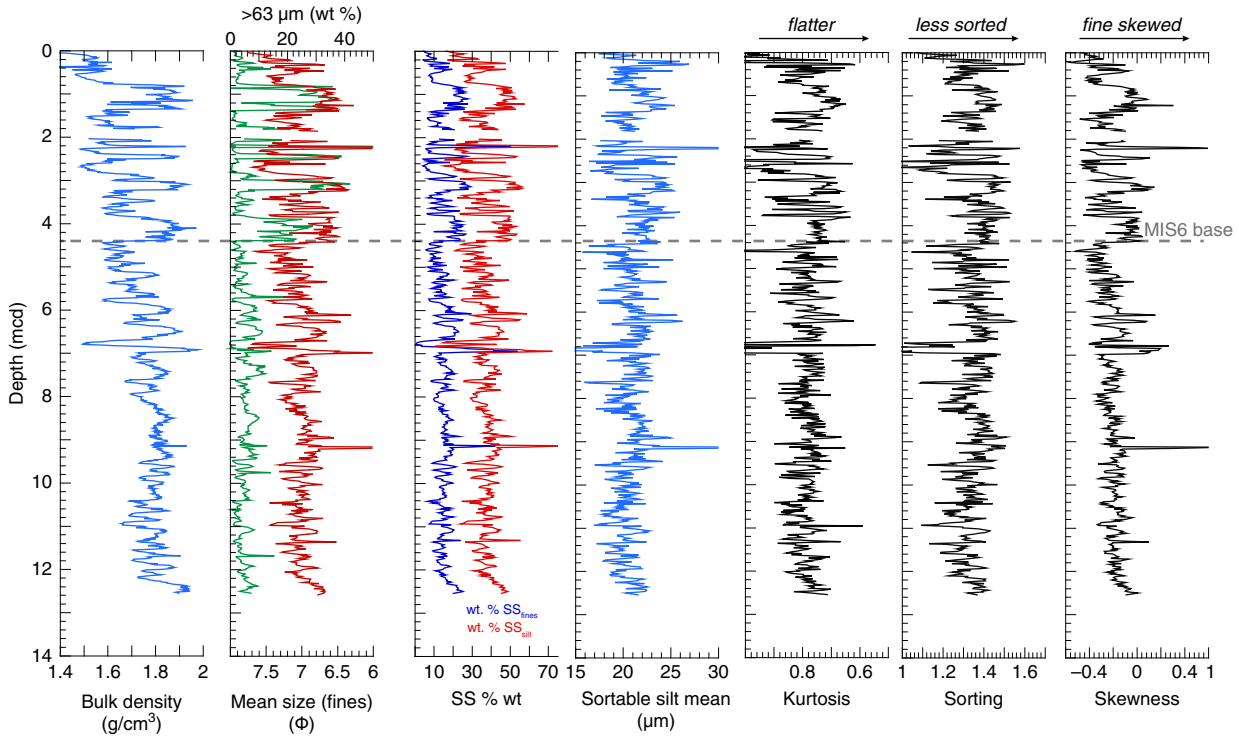

Fig. 3 Downhole plots of the bulk density, >63 μm % wt from sieving (green), mean size of the fines (red), SS % wt, sortable silt mean and the kurtosis, sorting and skewness calculated on the silt distributions.

Fig. 3). These offsets may arise from errors in the published age model, or slight offsets in the correlation between Core 18 and the ACEX record.

Above 4.4 mcd, which has consistently been interpreted as the base of MIS6 in sediment cores from the central Lomonosov Ridge (O'Regan 2011), there is a prominent change in the grain size pattern clearly evident by the higher amplitude variations in the >63 μm % wt content. These intervals are also considerably thicker than the less pronounced coarse units below 4.4 mcd (Fig. 3).

Sortable silt and coarse fraction variability

Bivariate plots of the SS % wt_{fines}, sortable silt mean and coarse fraction content in Core 18 illustrate a bias towards coarser silt grain sizes as the coarse fraction content increases (Fig. 5). Notably, samples with higher sortable silt mean and SS % wt_{fines} also have higher coarse fraction contents. Deviations from a near linear trend occur when the >63 μm % wt increases above 10%, which generally only occurs in sediments deposited from MIS6 to the present (Fig. 5).

In order to better visualize how the texture of the silt fraction changes as a function of the >63 μm % wt, frequency plots were generated for the fine fraction material in samples having coarse fraction contents of <5% wt, 5–10% wt and >10% wt (Fig. 6). The cumulative results are compared to samples older and younger than MIS6. In general, samples having >10% wt coarse fraction content, also have a more platykurtic (flatter) distribution of the fine fraction material. Conversely, samples with <5% wt coarse fraction content are skewed towards the fine silt and clay size fractions.

The relationship between statistical parameters describing the silt distribution (mean, sorting, skewness and kurtosis) and the >63 μm % wt of the sample are further illustrated by a series of bivariate plots (Fig. 7). These figures illustrate that distinct populations of samples do not clearly separate glacial and interglacial modes of sedimentation. Instead the frequency spectrums of the fine fraction material reveal a continuum where samples containing higher percentages of coarse fraction material also have a larger mean silt size, are more poorly sorted with a lower degree of kurtosis (flatter distribution) and are biased towards coarser silt sizes (i.e., fine skewed with a more positive skewness). Furthermore, the range and variability in the sorting, skewness and kurtosis, overlap with similar measurements performed on a series of sea-ice samples collected in Fram Strait (Fig. 7; Dethleff & Kuhlmann 2010). The largest discrepancy is that the sea-ice samples have a lower mean silt size than those from the sedimentary record.

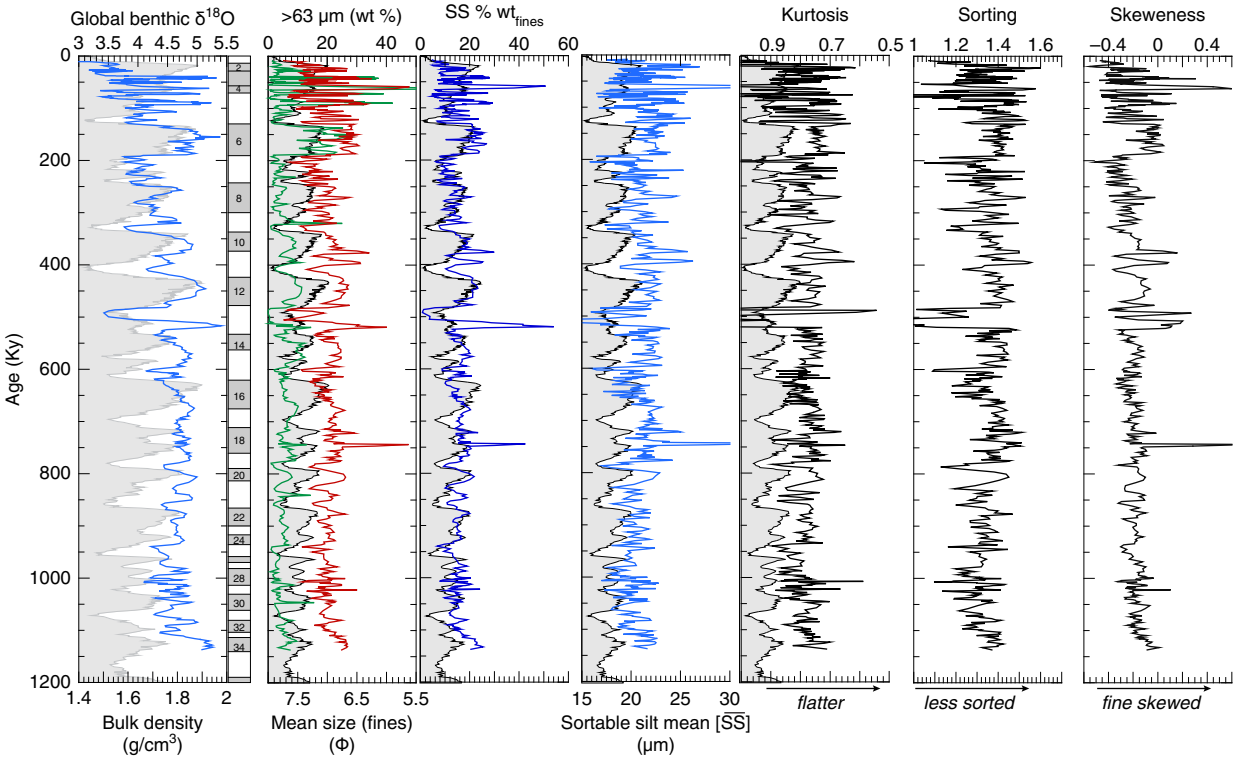

Fig. 4 Age-calibrated records of the parameters shown in Fig. 3 using the ACEX age model. The global stacked benthic d18O record of Lisiecki & Raymo (2005) is shown (grey-filled curve) in the background to help identify glacial and interglacial periods. Note that the reported uncertainties in the ACEX age model are large (illustrated in Fig. 2), and may, to some extent account for offsets between coarser grained intervals and glacial/stadial sediments.

Discussion

Detailed studies of the grain size distribution of the fine fraction are not common in the Arctic Ocean where there is a tendency to focus on the coarse fraction content of the sediment as a proxy for ice rafting. Coarse fraction data from the Quaternary section of the ACEX record, and other shorter sediment cores from the region (i.e., 96-12/1-PC, PS-2185-6; Fig. 1), reveal rather limited variation in the coarse fraction content of sediments prior to MIS6/7 (Jakobsson et al. 2001; Spielhagen et al. 2004; O'Regan et al. 2010). This contrasts with other long-term

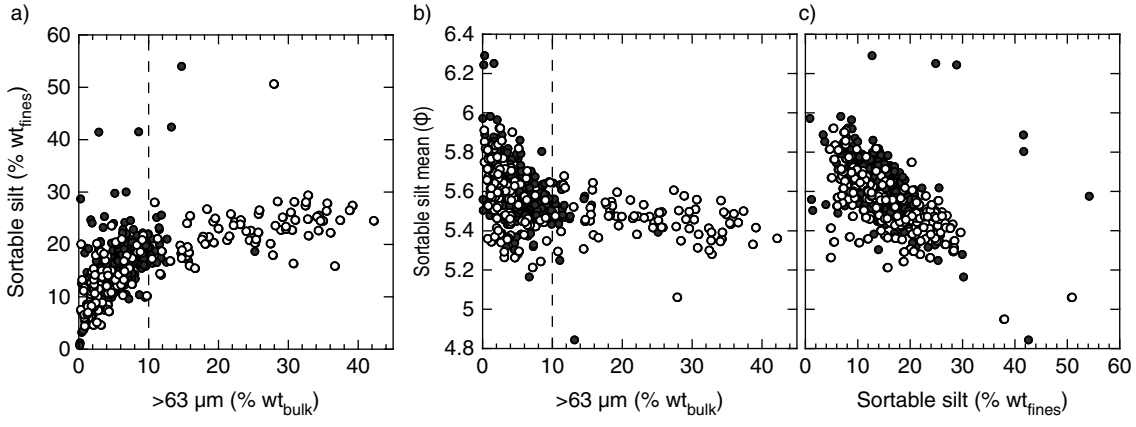

Fig. 5 Cross-plots of sortable silt parameters (SS % wt_{fines}, sortable silt mean) and the coarse fraction content (>63 μm % wt from sieving). (a) SS % wt_{fines} and >63 μm % wt (b) sortable silt mean and >63 μm % wt (c) sortable silt mean and SS % wt_{fines}. Black dots correspond to sediments older than MIS6 and grey dots sediments from MIS6 and younger.

Citation: *Polar Research* 2014, *33*, 23672, http://dx.doi.org/10.3402/polar.v33.23672

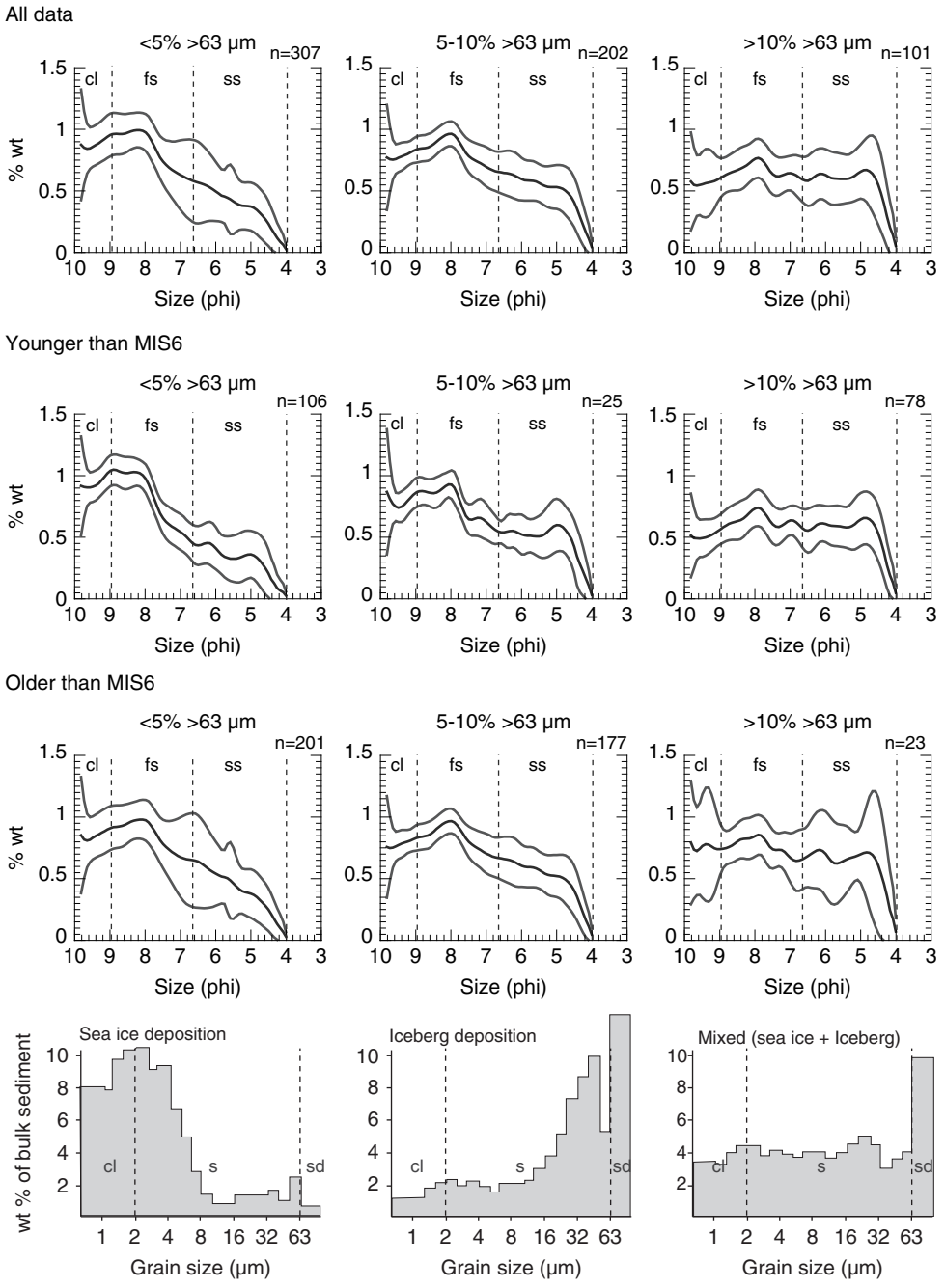

Fig. 6 Average size frequency plots for sediments from Core 18 (n is the number of samples averaged). All plots represent the 1–63 µm fractions presented in phi units. Frequency spectra are shown for all the data and compared to sediments from MIS 1–6 and older than MIS6. Spectra are subdivided into populations of samples having <5%, 5–10% and >10 wt % of coarse fraction material. The bottom pane illustrates interpreted modes of sediment texture related to sea ice and iceberg related deposition in the Arctic, and how they may combine to form a mixed sea ice–iceberg grain size signal (Clark & Hanson 1983). (Figure redrawn from Stein 2008.)

records recovered from the Norwegian and Greenland seas that reveal a clear increase in the abundance of coarse fraction content during Quaternary glacial periods as the Greenland, Barents and Scandinavian ice sheets developed (Polyak et al. 2010). These differences were tentatively explained by a more dominant sea ice control on deposition in the central Arctic Ocean, where iceberg related deposition played a relatively minor role in bulk sediment accumulation until the latest part of the Quaternary (O'Regan et al. 2010; Polyak et al. 2010).

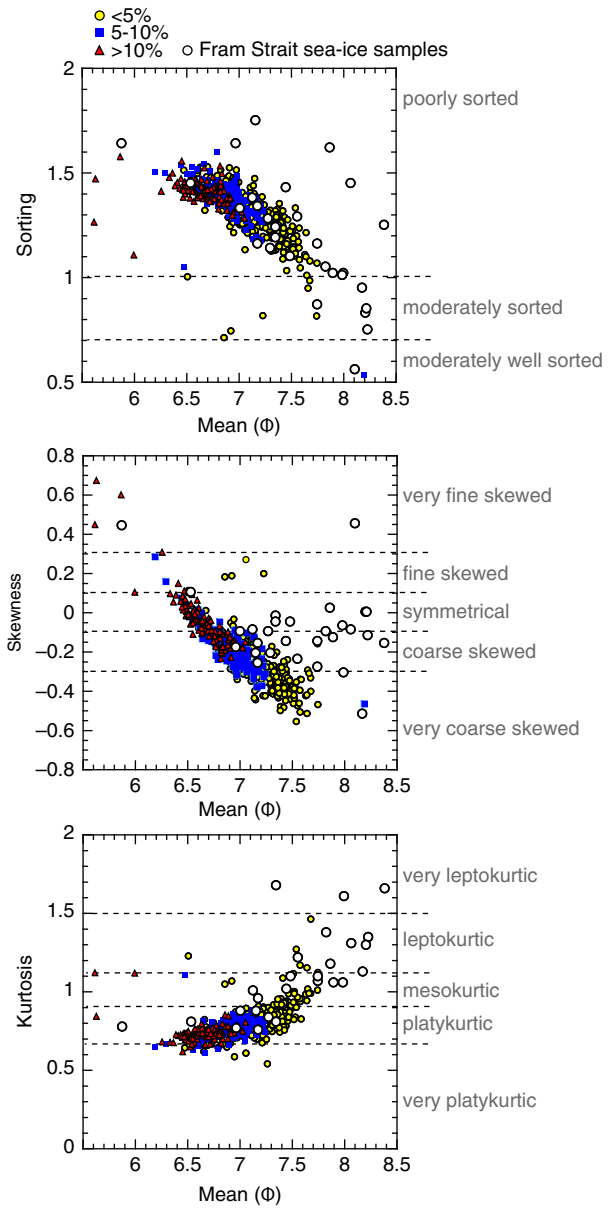

Fig. 7 Bivariate plots of silt statistical parameters, with samples coded depending on the % wt >63 μm; triangles ≤5%, squares = 5–10% and circles ≥10%. Overlain are results from a similar analysis conducted on 33 sea-ice samples from the Fram Strait (Dethleff & Kuhlmann 2010).

The abundance of >63 μm sediments in Core 18 reveals a similar trend to other records from the Lomonosov Ridge, with the most prominent coarse-grained intervals occurring during the last two glacial cycles. These intervals are associated with iceberg rafting events from the Barents–Kara ice sheet during MIS6, 5/4 and during the early period of MIS3 (Jakobsson et al. 2001; Spielhagen et al. 2004). The oldest of these intervals, deposited during MIS6, also coincides with dated glacial erosion of the 1000 m deep crest of the Lomonosov Ridge (Jakobsson 1999; Polyak et al. 2001), supporting the interpretation that these facies are likely related to iceberg deposition. However, even within these coarse-grained intervals (containing >10% wt of sand sized material), the frequency spectra remain more similar to the mixed sea-ice iceberg mode of deposition (Fig. 6).

The absence of similarly pronounced coarse-grained intervals in underlying sediments of Core 18, suggests a less pronounced influence by icebergs during glacial periods predating MIS6. Their absence has also complicated the clear identification of glacial–interglacial periods and the development of cyclostratigraphic-based age models. To this end, the more pronounced and higher frequency variation in the silt fraction identified by this study (Figs. 4, 5) provides a potential way to improve cyclostratigraphic analysis of central Arctic sediments.

The mean sortable silt size and SS % wt_{fines} have been successfully applied as palaeo-current proxies in the North Atlantic (McCave, Manighetti, & Beveridge 1995; Bianchi & McCave 1999). However, in regions more heavily influenced by sea ice, ice-rafted material complicates this interpretation. This is primarily due to the known bias towards the preferential enrichment of clays and silts within sea ice (Clark & Hanson 1983; Nürnberg et al. 1994; Reimnitz et al. 1998; Hebbeln 2000; Darby et al. 2009; Dethleff & Kuhlmann 2010). Hass (2002) has shown using a core collected from the western flank of Yermak Plateau that silt-sized material originating from sea ice has a significant influence on the sortable silt mean, and consequently, inferences made about current speeds. Here we also find in central Arctic sediments that the SS % wt_{fines} increases with >63 μm % wt content across the ca. 1 million year record of Core 18. Similarly, as the SS % wt_{fines} increases, the mean sortable silt increases (Fig. 6).

Recently, Hoffman et al. (2013) have suggested, based on ^{231}Pa and ^{230}Th burial in sediments from the Arctic, that the vigour of glacial and deglacial deepwater circulation in the Arctic was comparable to modern. Without considering the influence of sea-ice rafted sediments on the silt distributions, the increased sortable silt mean and larger SS % wt_{fines} during glacial periods in Core 18 could be interpreted as an enhanced current strength signal. However, the fact that intervals with higher SS % wt_{fines} and sortable silt mean are also more poorly sorted (Figs. 4 , 5), certainly suggests that coarsening during glacial periods is more likely related to a sea ice overprint and not enhanced deep water circulation.

A linear correlation between the wt % in different silt size bins with the >63 μm % wt reveals that it is primarily the coarse silt (>20 μm) that is positively correlated to the coarse fraction content (Fig. 8a). Comparison to the silt

Citation: *Polar Research* 2014, *33*, 23672, http://dx.doi.org/10.3402/polar.v33.23672

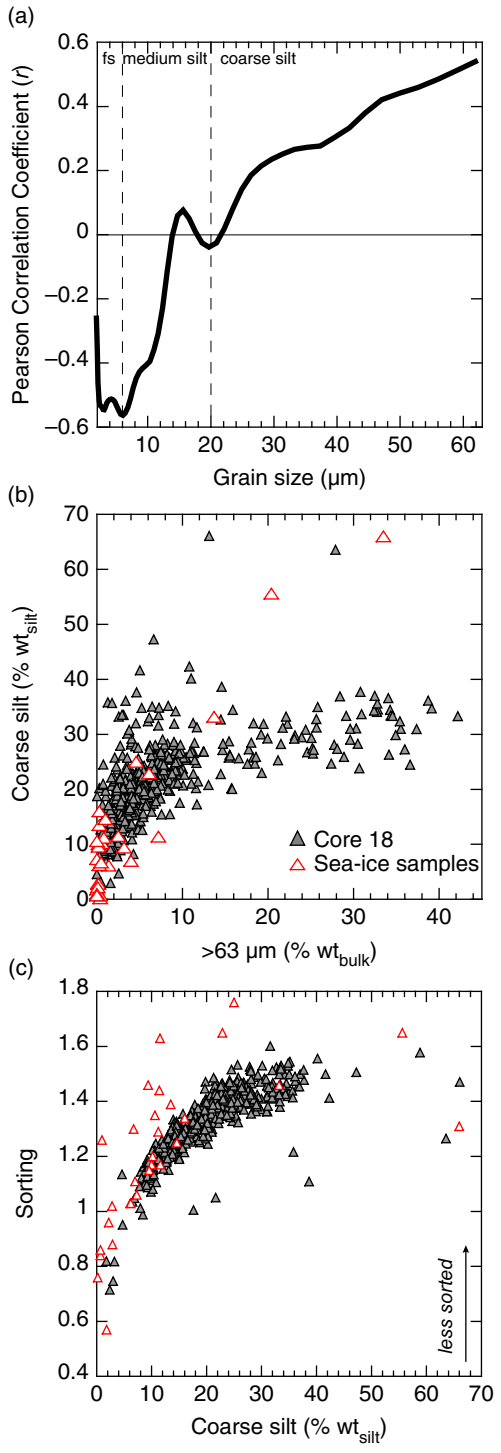

Fig. 8 (a) Linear correlation coefficients between % wt_{silt} in silt size bins and the >63 μm % wt from sieving. (b) Cross-plot of the coarse silt abundance (% wt_{silt}) and the >63 μm % wt from sieving. (c) Cross-plot of sorting of the silt fraction and the coarse silt abundance (% wt_{silt}) illustrating that intervals with higher abundances of coarse silt have less well sorted silt distributions. Overlain on (b) and (c) are results from sea-ice samples collected in Fram Strait (Dethleff & Kuhlmann 2010).

composition of sea ice samples from Fram Strait, shows a similar increase in the coarse silt (as a % wt_{silt}) as the >63 μm % wt increases (Fig. 8b). Since the >63 μm % wt in the sedimentary record is derived from ice rafting, a similar origin is implied for the coarse silt.

While our results illustrate that coarsening of fine fraction material accompanies an increase in the coarse fraction content, there remains some uncertainty as to how this signal is preserved and what drives the observed changes across glacial and interglacial cycles. There are three possible ways we envisage these changes occurring, none of which are mutually exclusive. The first is the delivery of more ice-rafted debris during glacial periods, which results in an overall coarsening of the sediment. However, except for the glacial/stadial stages between MIS 1–6, the current age model indicates lower relative sedimentation rates during glacial periods (O'Regan et al. 2008), which cannot be reconciled with increased coarse fraction input without reducing the input of fine fraction material. The observed reduction, or cessation, of sedimentation in the central Arctic during the Last Glacial Maximum provides an analogy to how a more stable perennial ice cover may reduce sedimentation in the Arctic during Quaternary glacial periods (Jakobsson et al. 2014). However, it should also be noted that the current age model precludes the detail needed to differentiate between glacial, deglacial and even interstadial periods, when more extensive ice melting would increase ice-rafted debris delivery to the seafloor.

A second method may be the cessation of fine fraction transport by either intermediate water currents or nepheloid layers (Rutgers van der Loeff et al. 2002). For example, an estimate, based on sediment traps on the southern Lomonosov Ridge near the Laptev Sea continental margin, indicates that over 60% of the lithogenic matter was laterally transported (Fahl & Nöthig 2007). It remains possible that fine silts and clays entrained along the continental slopes, are carried by deep waters to the central Lomonosov Ridge. If these currents are weakened during glacials (Cronin et al. 1995; Hebbeln & Wefer 1997; Matthiessen et al. 2001; Nørgaard-Pedersen et al. 2003), the deposition of fine fraction material would possibly be reduced, and result in the observed increase of the coarser grain sizes and generate a less diluted ice-drafted debris signal. Similarly, increased delivery of fine fraction material during interglacial/interstadial periods may occur as a consequence of the re-establishment of previously blocked north-flowing rivers that discharge into the Arctic Ocean (Mangerud et al. 2001).

A final possible explanation is that during glacial intervals, lowering of sea level allows either coarser grained sediment to be incorporated into sea ice via

suspension freezing, or there is a relative increase in the amount of anchor ice, which can incorporate a wider and coarser range of grain sizes (Reimnitz et al. 1987; Darby et al. 2011).

Testing these hypotheses requires additional analyses of the fine fraction material from stratigraphically aligned cores that today sit in different water masses. For example, while Core 18 sits in the Intra Basin where Arctic Deep Waters pass between the Makarov and Amundsen basins, cores from the crest of the Lomonosov Ridge are near the base of modern Arctic Intermediate Water. A comparative analysis of the fine fraction component from these different oceanographic settings may help identify vertical (ice-rafted debris) and lateral (current transported) inputs, and how they change across glacial and interglacial periods. To further isolate the sea-ice and iceberg related contribution to the silt distribution, analyses should extend to coarser size fractions. Finally, testing if sea-level variations across glacial and interglacial periods coarsen the silt distribution in Arctic sediments could be achieved by investigating sediments deposited prior to the establishment of large Northern Hemisphere ice sheets.

Summary and conclusions

This study provides a long-term perspective on middle to late Quaternary grain size variations within the fine fraction of sediments deposited on the Lomonosov Ridge. It uses the proposed ACEX age model to investigate how changes in the silt distribution of sediments changes between glacial and interglacial periods. The principal findings are that throughout the ca. 1 million year record, the SS % wt_{fines}, sortable silt mean, and coarse silt content all increase as the >63 μm % wt content increases. This appears to be similar to findings from modern sea ice samples and highlights the strong imprint that sea ice deposition has on the fine fraction distribution. As previously illustrated by Hass (2002), this ice-rafted overprint must be taken into account if the sortable silt is to be used as a proxy for past current speed. Finally, when compared to the coarse fraction content, larger amplitude and higher frequency changes seem to be preserved in the silt distributions of pre-MIS6 sediments. This more pronounced cyclicity may provide a way to improve age models in central Arctic sediments if it can be shown to be reproducible in other, stratigraphcially aligned cores.

Acknowledgements

The authors would like to thank the Swedish Research Secretariat, the captains and crews of the icebreakers USCGC *Healy* and *Oden* for their support during the HOTRAX expedition. This is a contribution from the Bert Bolin Centre of Climate Research at Stockholm University. Financial support was received from the Swedish Research Council (VR) and the Swedish Royal Academy of Sciences through a grant financed by the Knut and Alice Wallenberg Foundation.

References

Alexanderson H., Backman J., Cronin T.M., Funder S., Ingólfsson Ó., Jakobsson M., Landvik Jon Y., Löwemark L., Mangerud J., März C., Möller P., O'Regan M. & Spielhagen R.F. 2014. An Arctic perspective on dating Mid–Late Pleistocene environmental history. *Quaternary Science Reviews 92*, 9–31.

Backman J., Fornaciari E. & Rio D. 2009. Biochronology and paleoceanography of late Pleistocene and Holocene calcareous nanofossil abundances across the Arctic Basin. *Marine Micropaleontology 72*, 86–98.

Backman J., Jakobsson M., Løvlie R., Polyak L. & Febo L.A. 2004. Is the central Arctic Ocean a sediment starved basin? *Quaternary Science Reviews 23*, 1435–1454.

Bianchi G.G., Hall I.R., McCave I.N. & Joseph L. 1999. Measurement of the sortable silt current speed proxy using the Sedigraph 5100 and Coulter MultiSizer IIe: precision and accuracy. *Sedimentology 46*, 1001–1014.

Bianchi G.G. & McCave I.N. 1999. Holocene periodicity in North Atlantic climate and deep-ocean flow south of Iceland. *Nature 397*, 515–517.

Björk G., Jakobsson M., Rudels B., Swift J.H., Anderson L., Darby D.A., Backman J., Coakley B., Winsor P., Polyak L. & Edwards M. 2007. Bathymetry and deep-water exchange across the Lomonosov Ridge at 88°–89°N. *Deep-Sea Research Part I 54*, 1197–1208.

Blott S.J. & Pye K. 2001. GRADISTAT: a Grain size distribution and statistics package for the analysis of unconsolidated sediments. *Earth Surface Processes and Landforms 26*, 1237–1248.

Clark C.D. & Hanson A. 1983. Central Arctic sediment texture: a key to transport mechanisms. In B.F. Molnia (ed.): *Glacial–marine sedimentation*. Pp. 331–365. New York: Plenum Press.

Cronin T.M., Holtz J., Stein R., Spielhagen R.F., Fütterer D. & Wollenburg J. 1995. Late Quaternary paleoceanography of the Eurasian Basin, Arctic Ocean. *Paleoceanography 10*, 259–281.

Darby D., Jakobsson M., Polyak L. & HOTRAX Science Party 2005. Icebreaker expedition collects key Arctic seafloor and ice data. *Eos, Transactions of the American Geophysical Union 86*, 549, 552.

Darby D., Myers W.B., Jakobsson M. & Rigor I. 2011. Dirty sea ice characteristics and sources: the role of anchor ice. *Journal of Geophysical Research—Oceans 116*, C09008, doi: 10.1029/2010JC006675.

Darby D., Ortiz J., Polyak L., Lund S., Jakobsson M. & Woodgate R.A. 2009. The role of currents and sea ice in both slowly deposited central Arctic and rapidly deposited

Citation: *Polar Research* 2014, *33*, 23672, http://dx.doi.org/10.3402/polar.v33.23672

Chukchi–Alaskan margin sediments. *Global and Planetary Change 68*, 58–72.

Dethleff D. & Kuhlmann G. 2010. Fram Strait sea-ice sediment provinces based on silt and clay compositions identify Siberian Kara and Laptev seas as main source regions. *Polar Research 29*, 265–282.

Expedition 302 Scientists. 2006. Expedition 302 summary. In J. Backman et al. (eds.): *Proceedings of the integrated ocean drilling program 302*. Pp. 1–8. College Station, TX: Integrated Ocean Drilling Program Management International.

Fahl K. & Nöthig E.M. 2007. Lithogenic and biogenic particle fluxes on the Lomonosov Ridge (central Arctic Ocean) and their relevance for sediment accumulation: vertical vs. lateral transport. *Deep-Sea Research Part I 54*, 1256–1272.

Folk R.L. & Ward W.C. 1957. Brazos River bar: a study in the significance of grain size parameters. *Journal of Sedimentary Petrology 27*, 3–26.

Hanslik D., Jakobsson M., Backman J., Björck S., Sellén E., O'Regan M., Fornaciari E. & Skog G. 2010. Pleistocene Arctic Ocean sea ice and deep water isolation times. *Quaternary Science Reviews 29*, 3430–3441.

Hass H.C. 2002. A method to reduce the influence of ice-rafted debris on a grain size record from northern Fram Strait, Arctic Ocean. *Polar Research 21*, 299–306.

Hebbeln D. 2000. Flux of ice-rafted detritus from sea ice in the Fram Strait. *Deep-Sea Research Part II 47*, 1773–1790.

Hebbeln D. & Wefer G. 1997. Late Quaternary paleoceanography in the Fram Strait. *Paleoceanography 12*, 65–78.

Hoffman S.S., McManus J.F., Curry W.B. & Brown-Leger L.S. 2013. Persistent export of 231Pa from the deep central Arctic Ocean over the past 35,000 years. *Nature 497*, 603–606.

Jakobsson M. 1999. First high-resolution chirp sonar profiles from the central Arctic Ocean reveal erosion of Lomonosov Ridge sediments. *Marine Geology 154*, 111–123.

Jakobsson M., Andreassen K., Bjarnadóttir L.R., Dove D., Dowdeswell J.A., England J.H., Funder S., Hogan K., Ingólfsson Ó., Jennings A., Larsen N.K., Kirchner N., Landvik J.Y., Mayer L., Mikkelsen N., Möller P., Niessen F., Nilsson J., O'Regan M., Polyak L., Nørgaard-Pedersen N. & Stein R. 2014. Arctic Ocean glacial history. *Quaternary Science Reviews 92*, 40–67.

Jakobsson M., Løvlie R., Al-Hanbali H., Arnold E., Backman J. & Mörth M. 2000. Manganese and color cycles in Arctic Ocean sediments constrain Pleistocene chronology. *Geology 28*, 23–26.

Jakobsson M., Macnab R., Mayer M., Anderson R., Edwards M., Hatzky J., Schenke H.-W. & Johnson P. 2008. An improved bathymetric portrayal of the Arctic Ocean: implications for ocean modeling and geological, geophysical and oceanographic analyses. *Geophysical Research Letters 35*, LO7602, doi: 10.1029/2008GL033520.

Jakobsson M., Løvlie R., Arnold E.M., Backman J., Polyak L., Knudsen J.-O. & Musatov E. 2001. Pleistocene stratigraphy and paleoenvironmental variation from Lomonosov Ridge sediments, central Arctic Ocean. *Global and Planetary Change 31*, 1–22.

Jones E.P. 2001. Circulation of the Arctic Ocean. *Polar Research 20*, 139–146.

Lisiecki L.E. & Raymo M.E. 2005. A Pliocene–Pleistocene stack of 57 globally distributed benthic $\delta^{18}O$ records. *Paleoceanography 20*, PA 1003, doi: 10.1029 2004PA001071.

Löwemark L., O'Regan M., Hanebuth T.J.J. & Jakobsson M. 2012. Late Quaternary spatial and temporal variability in Arctic deep-sea bioturbation and its relation to Mn cycles. *Palaeogeography, Palaeoclimatology, Palaeoecology 365–366*, 192–208.

Mangerud J., Astakhov V., Jakobsson M. & Svendsen J.I. 2001. Huge ice-age lakes in Russia. *Journal of Quaternary Science 16*, 773–777.

Matthiessen J., Knies J., Nowaczyk N.R. & Stein R. 2001. Late Quaternary dinoflagellate cyst stratigraphy at the Eurasian continental margin, Arctic Ocean: indications for Atlantic Water inflow in the past 150,000. *Global and Planetary Change 31*, 65–86.

McCave I.N. & Hall I.R. 2006. Size sorting in marine muds: processes, pitfalls, and prospects for paleoflow-speed proxies. *Geochemistry Geophysics Geosystems 7*, article no. Q10N05, doi: 10.1029/2006GC001284.

McCave I.N., Hall I.R. & Bianchi G.G. 2006. Laser vs. settling velocity differences in silt grainsize measurements: estimation of palaeocurrent vigour. *Sedimentology 53*, 919–928.

McCave I.N., Manighetti B. & Beveridge N.A.S. 1995. Circulation in the glacial North-Atlantic inferred from grain-size measurements. *Nature 374*, 149–152.

McCave I.N., Manighetti B. & Robinson S.G. 1995. Sortable silt and fine sediment size/composition slicing: parameters for palaeocurrent speed and palaeoceanography. *Paleoceanography 10*, 593–610.

Nørgaard-Pedersen N., Spielhagen R.F., Erlenkeuser H., Grootes P.M., Heinemeier J. & Knies J. 2003. Arctic Ocean during the Last Glacial Maximum: Atlantic and polar domains of surface water mass distribution and ice cover. *Paleoceanography 18*, article no. 1063, doi: 10.1029/2002PA 000781.

Nürnberg D., Wollenburg J., Dethleff D., Eicken H., Kassens H., Letzig T., Reimnitz E. & Thiede J. 1994. Sediments in Arctic sea ice: implications for entrainment transport and release. *Marine Geology 119*, 184–214.

O'Regan M. 2011. Late Cenozoic Paleoceanography of the Central Arctic Ocean. *IOP Conference Series: Earth and Environmental Science 14*, article no. 012002, doi: 10.1088/ 1755-1315/14/1/012002.

O'Regan M., King J., Backman J., Jakobsson M., Pälike H., Moran K., Heil C., Sakamoto T., Cronin T. & Jordan R. 2008. Constraints on the Pleistocene chronology of sediments from the Lomonosov Ridge. *Paleoceanography 23*, PA1S19, doi: 10.1029/2007PA001551.

O'Regan M., St. John K., Moran K., Backman K., King J., Haley B.A., Jakobsson M., Frank M. & Röhl U. 2010. Plio-Pleistocene trends in ice rafted debris on the Lomonosov Ridge. *Quaternary International 219*, 168–176.

Pfirman S., Wollenburg I., Thiede J. & Lange M.A. 1989. Lithogenic sediment on Artic pack ice: potential aeolian flux

and contributions to deep sea sediments. In M. Sarnthein & M. Leinen (eds.): *Paleoclimatology and paleometeorology: modern and past pattern of global atmospheric transport*. Pp. 463–493. Dordrecht: Kluwer.

Polyak L., Alley R.B., Andrews J.T., Brigham-Grette J, Cronin T.C., Darby D., Dyke A.S., Fitzpatrick J.J., Funder S., Holland M., Jennings A.E., Miller G.H., O'Regan M., Savelle J., Serreze M., St. John K., White J.W.C. & Wolff E. 2010. History of sea ice in the Arctic. *Quaternary Science Reviews 29*, 1757–1778.

Polyak L., Edwards M.H., Coakley B.J. & Jakobsson M. 2001. Ice shelves in the Pleistocene Arctic Ocean inferred from glaciogenic deep-sea bedforms. *Nature 410*, 453–457.

Reimnitz E., Kempema E.W. & Barnes P.W. 1987. Anchor ice, seabed freezing, and sediment dynamics in shallow Arctic seas. *Journal of Geophysical Research—Oceans 92*, 14671–14678.

Reimnitz E., McCormick M., Bischof J. & Darby D.A. 1998. Comparing sea ice sediment load with Beaufort Sea shelf deposits: is entrainment selective? *Journal of Sedimentary Research 68*, 777–787.

Rudels B., Anderson L., Eriksson P., Fahrbach E., Jakobsson M., Jones E.P., Melling H., Prinsenberg S., Schauer U. & Yao T. 2012. Observations in the ocean. In P. Lemke (ed.): *Arctic climate change: the ACSYS decade and beyond. Vol. 43*. Pp. 117–198. Dordrecht: Springer.

Rutgers van der Loeff M.M., Meyer R., Rudels B. & Rachor E. 2002. Resuspension and particle transport in the benthic nepheloid layer in and near Fram Strait in relation to faunal abundances and ^{234}Th depletion. *Deep-Sea Research Part I 49*, 1941–1958.

Sellén E., O'Regan M. & Jakobsson M. 2010. Spatial and temporal Arctic Ocean depositional regimes: a key to the evolution of ice drift and current patterns. *Quaternary Science Reviews 29*, 3644–3664.

Spielhagen R.F., Baumann K.H., Erlenkeuser H., Nowaczyke N.R., Nørgaard-Pedersen N., Vogt C. & Weiel D. 2004. Arctic Ocean deep-sea record of northern Eurasian ice sheet history. *Quaternary Science Reviews 23*, 1455–1483.

Stein R. 2008. *Arctic Ocean sediments: processes, proxies, and paleoenvironment*. Amsterdam: Elsevier.

Stein R., Fahl K. & Müller J. 2012. Proxy reconstructions of Cenozoic Arctic Ocean sea-ice history—from IRD to IP_{25}–. *Polarforschung 82*, 37–71.

Xuan C., Channell J.E.T., Polyak L. & Darby D.A. 2012. Paleomagnetism of Quaternary sediments from Lomonosov Ridge and Yermak Plateau: implications for age models in the Arctic Ocean. *Quaternary Science Reviews 32*, 48–63.